

Quasiregularity and rigorous diffusion of strong Hamiltonian chaos

O. Barash and I. Dana

Minerva Center and Department of Physics, Bar-Ilan University, Ramat-Gan 52900, Israel

(Received 8 June 2006; published 6 November 2006)

Exact results are derived concerning quasiregularity and diffusion of strong chaos on resonances of the sawtooth map. A chaotic ensemble of well-defined quasiregularity type (the sequence of resonances visited) is generally a fractal set whose main characteristics, the topological entropy and the Hausdorff dimension, are calculated exactly, under some conditions, using a symbolic dynamics. The effect of quasiregularity on chaotic diffusion is characterized by an infinity of diffusion coefficients, each associated with a fractal ensemble trapped in a periodic set of resonances. In some cases, these coefficients are calculated exactly and it is shown that rigorous diffusion takes place on the resonances.

DOI: [10.1103/PhysRevE.74.056202](https://doi.org/10.1103/PhysRevE.74.056202)

PACS number(s): 05.45.Ac, 05.45.Mt, 45.05.+x

I. INTRODUCTION

Typical Hamiltonian systems exhibit regular and chaotic motions intricately mixed on all scales of phase space. The regular-motion components usually have a strong impact on the chaotic dynamics. In particular, the stickiness of chaotic orbits to the boundaries of stability islands leads to long-time correlations in an ensemble of such orbits [1–3]. It is therefore not clear yet to precisely what extent chaos, in the presence of regular motion, is close to a purely random process, featuring statistical properties such as diffusion. In this paper, we derive exact results concerning strongly chaotic diffusion in a Hamiltonian system having no stability islands but whose dynamics is highly nontrivial and contains unstable regular-motion components. This is the well-known sawtooth map (SM) on a cylindrical phase space:

$$M: p_{t+1} = p_t + Kf(x_t), \quad x_{t+1} = x_t + p_{t+1} \pmod{1}, \quad (1)$$

where p is angular momentum, x is the angle, K is a nonintegrability positive parameter, and $f(x)$ is a sawtooth function: $f(x) = x - 1/2$ for $0 < x < 1$, $f(0) = 0$, and $f(x+1) = f(x)$. The SM is a uniformly hyperbolic and completely chaotic system. It was apparently first introduced by Rokhlin [4] and it continued to attract attention until these very days [5–20]. Nonsmooth systems such as the SM are, in principle, experimentally realizable [21] like the smooth ones. The SM also describes approximately, or is closely related to, several realistic systems, e.g., the standard map [map (1) with $f(x) = \sin(2\pi x)/(2\pi)$] in its strong-chaos (large K) regime and the stadium (Bunimovich) billiard [17]. The “elliptic” SM, with $-4 < K < 0$, exhibits remarkable phenomena [2,22,23], such as “pseudochaos.” Recently [19,20], the quantized SM was used to demonstrate the enormous efficiency of quantum computers in simulating complex quantum dynamics. Despite its apparent simplicity, the SM features a very nontrivial symbolic dynamics and a rich variety of unstable orbit structures [9–13]. Some of these structures are quite analogous to those exhibited by typical Hamiltonian systems with a mixed phase space. A prominent example are the rotational resonances built, as in the case of generic maps (1), on ordered (Poincaré-Birkhoff) periodic orbits [3,26,27]; the resonances are the basic regular-motion components of the SM and give an exact partition of phase space [11–13] (see a

summary in Sec. II). Because of this partition, a general chaotic orbit must be a sequence of quasiregular segments inside resonances; this sequence defines the “type” of the orbit [13,14] (see Sec. III).

Diffusion in the p direction is characterized by the global diffusion coefficient $D = \lim_{t \rightarrow \infty} \langle (p_t - p_0)^2 \rangle_{\mathcal{E}} / (2t)$, where $\langle \rangle_{\mathcal{E}}$ denotes average over an ensemble \mathcal{E} of initial conditions (x_0, p_0) in phase space. For sufficiently small K , $D(K)$ appears to scale as $K^{2.5}$, a behavior well reproduced by a Markov model of transport based on the resonances [11]. This scaling seems to be generic for discontinuous systems [17,18]. Several results have been obtained in the case of integer K (“cat maps”) [8,15,23–25]. In particular, if \mathcal{E} is chosen as the entire torus $0 \leq x, p < 1$, the value of D in this case is exactly calculable [8]: $D = K^2/24$. This value is reproduced also by finite ensembles \mathcal{E} of periodic orbits of given period T as $D = \langle (p_T - p_0)^2 \rangle_{\mathcal{E}} / (2T)$ [15].

In Sec. II, we summarize known facts about the rotational resonances of the SM. We then derive exact results concerning chaotic ensembles having a well-defined quasiregularity type (Sec. III) and ensembles \mathcal{G} trapped in some periodic set \mathcal{S} of resonances in the p direction (Sec. IV); see also Ref. [13]. All these ensembles are generally fractal sets whose main characteristics (topological entropy and Hausdorff dimension) are calculated exactly, under some conditions, using a convenient symbolic dynamics which we introduce. The ensemble \mathcal{G} is also characterized by a diffusion coefficient $D_{\mathcal{G}}$ which is calculated exactly in the case that all the resonances in \mathcal{S} have the same order. We show that in this case one has a rigorous diffusion of \mathcal{G} on \mathcal{S} . These exact results hold for all K larger than some threshold value, i.e., they are not limited to specific (e.g., integer) K values. The coefficients $D_{\mathcal{G}}$ characterize the effect of quasiregularity on chaotic diffusion in much more detail than the single global coefficient D . A summary and conclusions are presented in Sec. V.

II. ROTATIONAL RESONANCES IN THE SM

In this section, we briefly summarize known facts about the SM rotational resonances (see more details in Ref. [12]). We first recall the important concept of ordered (Poincaré-Birkhoff) orbits [26,27]. To a sequence of orbit angles x_t ,

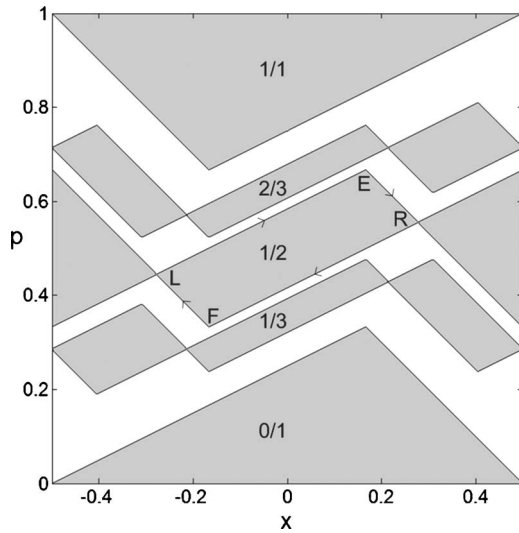


FIG. 1. SM resonances $\nu=0/1, 1/3, 1/2, 2/3,$ and $1/1$ for $K=0.5$. The hyperbolic ordered PO, on which a resonance is built, consists of the “X” points connecting neighboring zones of the resonance. The principal zone (such as the zone $LERF$ in the principal gap LR for $\nu=1/2$) is always symmetrically positioned around $x=0$. The vector \overline{LE} (\overline{ER}) is parallel to the unstable (stable) eigenvector \mathbf{E}_u (\mathbf{E}_s).

there corresponds its “lifted” sequence \tilde{x}_t obtained by using the map (1) with the mod(1) removed. An orbit of (1) is ordered like a rotation if it possesses the order-preserving (or monotonicity) property $\tilde{x}_t+a < \tilde{x}_{t'} \Leftrightarrow \tilde{x}_{t+1}+a < \tilde{x}_{t'+1}$ for all integers a, t, t' . For an ordered periodic orbit (PO) with minimal period n , one has $p_{t+n}=p_t$ and $x_{t+n}=x_t$ or $\tilde{x}_{t+n}=\tilde{x}_t+m$, where m is integer and (m, n) are coprime. The winding number $\nu=m/n$ gives an average value of p for the PO. One defines a “gap” \mathbf{G} as a pair of PO points having neighboring values of x_t ; the “principal” gap \mathbf{G}_0 is the pair of points with x_t closest to $x=0$ (such as the points L and R in Fig. 1). The n gaps of the ordered PO can be shown to be precisely the n iterates $\mathbf{G}_t=M^t\mathbf{G}_0$ of $\mathbf{G}_0, t=0, \dots, n-1$; also, \mathbf{G}_{t+1} is separated from \mathbf{G}_t by $|m|-1$ gaps. For $K=0$ (purely rotation map), all the orbits are ordered. For $K>0$ and arbitrary given rational m/n , the SM has one ordered PO with $\nu=m/n$ and \mathbf{G}_0 symmetrically positioned around the discontinuity line $x=0$. Thus, no PO point lies on $x=0$, so that the PO is fully hyperbolic. In fact, except of orbits with points on $x=0$, the SM is uniformly hyperbolic, i.e., its linearization is a constant 2×2 matrix with eigenvalues $\lambda=1+(K+\sqrt{K^2+4K})/2$ and λ^{-1} . The corresponding “unstable” and “stable” eigenvectors are given, respectively, by $\mathbf{E}_u=(1, 1-\lambda^{-1})$ and $\mathbf{E}_s=(1, 1-\lambda)$, where the first (second) component is in the (p) direction.

The $\nu=m/n$ resonance is then built on the ordered PO above as follows. Consider in Fig. 1 (for $\nu=1/2$) the parallelogram $\mathcal{Z}^{(0)}(\nu)=LERF$ made by connecting the two points L and R of \mathbf{G}_0 by segments parallel to \mathbf{E}_u and \mathbf{E}_s . The m/n resonance is defined as the chain of n “zones” (parallelograms) $\mathcal{Z}^{(s)}(\nu)=M^{-s}\mathcal{Z}^{(0)}(\nu), s=0, \dots, n-1$; each zone lies in some gap of the PO and $\mathcal{Z}^{(0)}(\nu)$ is the principal zone of the resonance. In Fig. 1, we show some examples of resonances

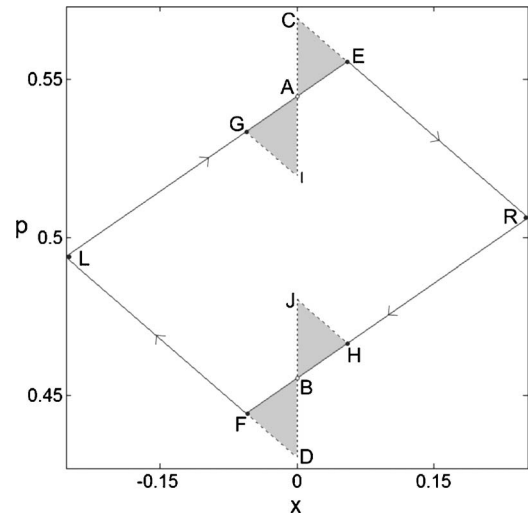


FIG. 2. Principal zone (solid lines) of resonance $\nu=1/2$ for $K=0.05$ with its upper and lower turnstiles (shaded regions).

built in the way above. The resonances for all m/n do not overlap and give an exact partition of phase space [12].

Clearly, the zone $\mathcal{Z}^{(n)}(\nu)=M^{-n}\mathcal{Z}^{(0)}(\nu)$ (the region $LGICRHJDL$ in Fig. 2) lies again in the principal gap. This zone differs from $\mathcal{Z}^{(0)}(\nu)$ by two “turnstiles” (the shaded regions in Fig. 2), each consisting of two triangular lobes of equal area touching at one point. By construction, the lobes inside (outside) $\mathcal{Z}^{(0)}(\nu)$ form the region exiting (entering) the resonance in one iteration. As K (and thus λ) is increased, the size of the turnstiles increases until eventually, when $\lambda^n > 3$ [12], one lobe of the upper turnstile begins to overlap with one lobe of the lower turnstile ($p_I < p_B$ and $p_J > p_A$; see Fig. 3). Then, the region exiting the resonance to below (above) is not a triangle but actually the trapezoid $\bar{V}_0=BAMH$ ($\bar{V}_1=ABNG$). Similarly, the region entering the resonance from below (from above) is the trapezoid $DFNI$ ($CEMJ$).

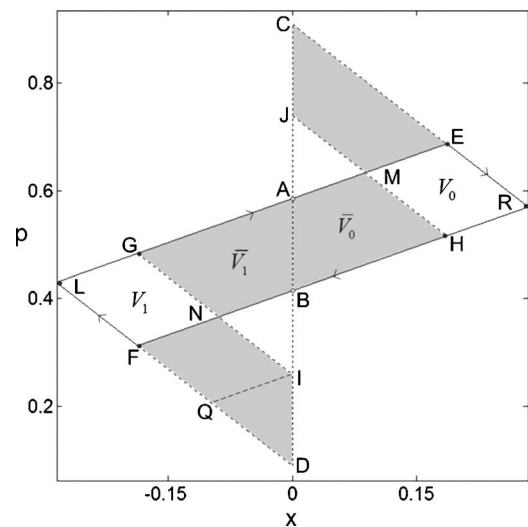


FIG. 3. Principal zone (solid lines) of resonance $\nu=1/2$ for $K=0.65$ with its generalized turnstiles (shaded regions); see text for more details.

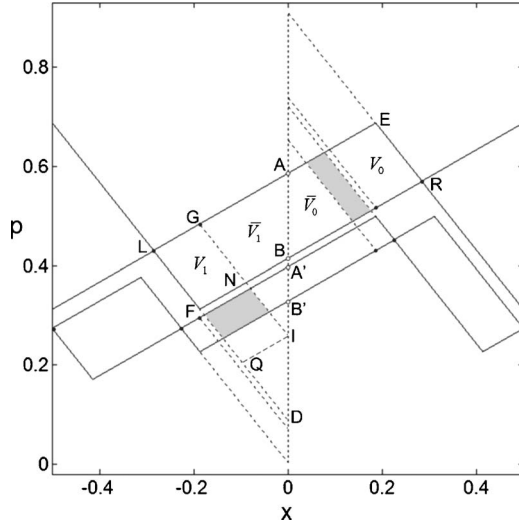


FIG. 4. Resonances $\nu=1/2$ and $\nu'=1/3$ (solid lines) for $K=0.65$ with their generalized turnstiles and the TOs (shaded regions); see text for more details.

Thus, for $\lambda^n > 3$, one has to define “generalized” turnstiles: the lower (upper) generalized turnstile consists of the lobes $BAMH$ and $DFNI$ (the lobes $ABNG$ and $CEMJ$). The parallelograms $V_0=MERH$ and $V_1=LGNF$ are the nonescaping regions of $LERF$ under one iteration of M^n [28].

Given two resonances $\nu=m/n$ and $\nu'=m'/n'$, the entering lobe of a turnstile of ν may overlap with the exiting lobe of a turnstile of ν' and vice versa. Figure 4 shows an example of these overlaps (shaded) for $\nu > \nu'$ and generalized turnstiles. The overlaps give the regions transferred from one resonance to another in one iteration. It turns out that there are only five distinct cases of turnstile overlap (TO) [12], depending on the value of K . The most important case for the purposes of this paper is that of a TO whose shape is a parallelogram, illustrated in Fig. 4. Such a shape can arise only for generalized turnstiles when $p_1 \leq p_{B'}$, or $AI \geq AB'$. The latter condition can be written more explicitly using $AI=K/2$ [12] and $AB'=|p_\nu - p_{\nu'}| + (AB + A'B')/2$, where p_ν and $p_{\nu'}$ denote the p coordinates of the centers of the principal zones $\mathcal{Z}^{(0)}(\nu)$ and $\mathcal{Z}^{(0)}(\nu')$; the “height” AB of ν is given by $AB=K/(\lambda^n - 1)$ [12]. Then, $AI \geq AB'$ is equivalent to

$$K \geq 2|p_\nu - p_{\nu'}| + \frac{K}{\lambda^n - 1} + \frac{K}{\lambda^{n'} - 1}. \quad (2)$$

III. ENSEMBLES WITH WELL-DEFINED QUASIREGULARITY TYPE

The exact resonance partition of phase space in the SM implies that a general orbit (except of a zero-measure set of orbits, e.g., cantori) must have all its points within resonances and must therefore perform a quasiregular motion as follows. Suppose that the initial point of the orbit lies in zone $\mathcal{Z}^{(s)}(\nu) = M^{-s}\mathcal{Z}^{(0)}(\nu)$ of resonance ν for some $s=0, \dots, n-1$. Then, after s iterations, it will lie in the principal zone

$\mathcal{Z}^{(0)}(\nu)$. If it does not lie in an exiting turnstile lobe, it will visit again the n zones of ν , returning to $\mathcal{Z}^{(0)}(\nu)$ after n iterations. If, on the other hand, it lies in an exiting turnstile lobe, more precisely in the TO of ν with resonance $\nu'=m'/n'$, it will escape to zone $\mathcal{Z}^{(n'-1)}(\nu')$ and it will perform at least a finite number of rotations (of n' iterations each) in ν' before escaping to another resonance. Thus, a general orbit is a sequence of quasiregular segments, each lying in some resonance $\nu_r = m_r/n_r$, $-\infty < r < \infty$, and having a length of $q_r n_r$ iterations, where q_r is the number of rotations performed in ν_r . We denote this sequence by $\tau = \dots, (\nu_r)_{q_r}, (\nu_{r+1})_{q_{r+1}}, \dots$, and we say that the orbit is of type τ .

The chaotic region can be well approximated by the ensemble of all POs with sufficiently large period. A general PO of (1) is defined by $p_{t+T} = p_t + P$ and $x_{t+T} = x_t$, where the period T is the smallest positive integer such that the last equations are satisfied for some integer P . If $P \neq 0$, the PO is an accelerator mode. The type τ of a PO must have the form $\tau = \dots, \Gamma(-P_\tau), \Gamma(0), \Gamma(P_\tau), \Gamma(2P_\tau), \dots$, where $\Gamma(uP_\tau)$ (u and P_τ are integers and P_τ is related to P ; see below) is a basic (primitive) “block” involving a finite number R of resonances, $\Gamma(uP_\tau) = (\nu_1 + uP_\tau)_{q_1}, \dots, (\nu_R + uP_\tau)_{q_R}$. The R resonances ν_1, \dots, ν_R may not be all different. Generally, the periodic cycle of the PO is completed only after visiting the block Γ more than one time, say l times. Then, $T = lT_\tau$, where $T_\tau = \sum_{r=1}^R q_r n_r$, and $P = lP_\tau$. We denote by $\mathcal{U}_{\tau,l}$ and $N(\tau, l)$, respectively, the ensemble and number of all POs of type τ and periods $T' = l'T_\tau$, where l' divides l (including $l' = l$). For a completely chaotic ensemble such as $\mathcal{U}_{\tau,l}$, one expects an exponential increase of $N(\tau, l)$ with l . We then associate with $\mathcal{U}_\tau = \cup_l \mathcal{U}_{\tau,l}$ the topological entropy

$$h_\tau = \lim_{l \rightarrow \infty} \frac{\ln[N(\tau, l)]}{lT_\tau}. \quad (3)$$

As $l \rightarrow \infty$ or $T_\tau \rightarrow \infty$, $\mathcal{U}_{\tau,l}$ approaches an ensemble \mathcal{C}_τ of aperiodic chaotic orbits.

We now study the orbits of type τ involving a finite number R of basic resonances, as above, under the condition that any two consecutively visited resonances, ν_r and ν_{r+1} ($\nu_{r+1} \equiv \nu_r + P_\tau$), have a parallelogram TO, i.e., relation (2) is satisfied for $\nu = \nu_r$ and $\nu' = \nu_{r+1}$. We then show below that an orbit of type τ is uniquely determined by a bi-infinite binary symbol sequence $\{c\}_\tau = \dots, c_{i-1}, c_i, \dots$ ($c_i = 0, 1$) whose general structure is as follows (using the notation $C_\tau = \sum_{r=1}^R q_r$): If $i = q_r \bmod (C_\tau)$ (i.e., $i = q_r + gC_\tau$ for some $r = 1, \dots, R$ and for some integer g), then c_i is fixed by τ , namely $c_i = 0$ for $\nu_{r+1} < \nu_r$ and $c_i = 1$ for $\nu_{r+1} > \nu_r$; otherwise [$i \neq q_r \bmod (C_\tau)$], c_i is arbitrary, i.e., it assumes the values $c_i = 0, 1$ independently. In particular, for a PO in $\mathcal{U}_{\tau,l}$, $\{c\}_\tau$ is periodic with period lC_τ ; lR symbols are fixed by τ as above and lQ_τ symbols are independent, where $Q_\tau \equiv C_\tau - R = \sum_{r=1}^R q_r - R$. Thus, one has $N(\tau, l) = 2^{lQ_\tau}$, so that from (3) we get

$$h_\tau = \frac{Q_\tau \ln(2)}{T_\tau}. \quad (4)$$

If $Q_\tau = 0$, i.e., $q_r = 1$ for all $r = 1, \dots, R$, $h_\tau = 0$ in (4). In fact, in this case there exists only one orbit of type τ , a PO with period $T = T_\tau$.

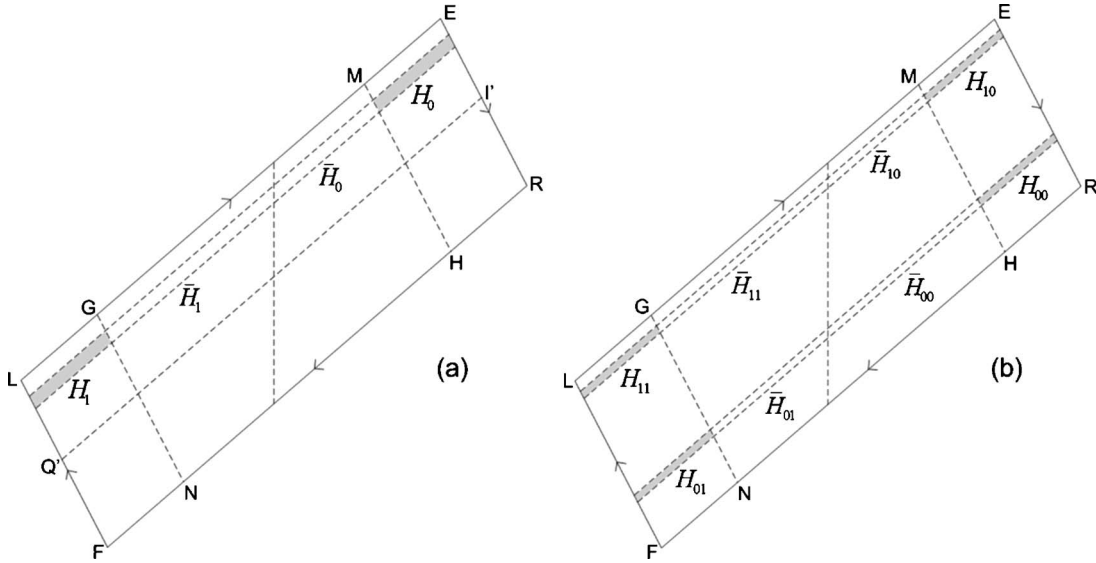


FIG. 5. Schematic illustration of the principal zone (solid lines) of a resonance, showing several regions defined in the text (see more details there): (a) the regions H_0 and H_1 (shaded) and the regions \bar{H}_0 and \bar{H}_1 , separated by the discontinuity line (the vertical dashed line); the union of these four regions is the h strip H . (b) The regions $H_{c,c'}$ (shaded) and $\bar{H}_{c,c'}$ for $c, c'=0, 1$.

We also show below that the initial conditions for all the orbits of type τ form a horseshoe \mathcal{H}_τ i.e., an invariant fractal set whose Hausdorff dimension \bar{D}_τ is given by

$$\bar{D}_\tau = \frac{2Q_\tau \ln(2)}{T_\tau \ln(\lambda)} = \frac{2h_\tau}{\ln(\lambda)}. \quad (5)$$

To show all this, we first note that initial conditions for all orbits of type τ can be found in one TO. We denote the TO between ν_r and ν_{r+1} ($\nu_{r+1} \equiv \nu_1 + P_\tau$) by $O_{r,r+1}$. Without loss of generality, we assume that $P_\tau=0$ [29] and we start from the TO $O_{R,1}$, which is mapped inside $\mathcal{Z}^{(0)}(\nu_1)$ under M^{n_1} . For the sake of illustration, we assume that ν_1 and ν_R are represented, respectively, by the upper and lower resonance in Fig. 4; then, $O_{R,1}$ is the lower TO in Fig. 4, crossing the left part of $\mathcal{Z}^{(0)}(\nu_R)$. For simplicity, we change temporarily the notation, $\nu_1, n_1 \rightarrow \nu, n$. The zone $\mathcal{Z}^{(0)}(\nu) = LERF$ is shown in more detail in Fig. 3. It is clear from the end of Sec. II that the parallelogram $LGIQ$ is mapped inside $LERF$ under M^n and its area is less than half of that of $LERF$. Using also the facts that \mathbf{E}_u (\mathbf{E}_s) expands (contracts) by a factor of λ^n under M^n and that $LG=FN=\lambda^{-n}LE$ [12], we see that $LGIQ$ is actually mapped under M^n into the parallelogram $LEI'Q'$ [see Fig. 5(a)]. Thus, the lower TO in Fig. 4 is mapped under M^n into the dashed “horizontal” (h) strip parallel to LE in Fig. 5(a). We denote this strip by H and we define, for $c=0, 1$, the regions $H_c = H \cap V_c$ [shaded in Fig. 5(a)] and $\bar{H}_c = H \cap \bar{V}_c$. Then, for $c=0, 1$, $M^n H_c$ are clearly the two dashed h strips parallel to LE in Fig. 5(b); $M^n H_1$ is closer to LE than H while $M^n H_0$ lies in the lower half of $LERF$, since $\lambda^n > 3$. In Fig. 5(b) we indicate, for $c, c'=0, 1$, the regions $H_{c,c'} = (M^n H_c) \cap V_{c'}$ (shaded) and $\bar{H}_{c,c'} = (M^n H_c) \cap \bar{V}_{c'}$. In general, denoting an arbitrary binary symbol sequence segment of length q by $\{c\}_q = c_1, \dots, c_q$, one generates 2^q h strips $H_{\{c\}_q}$ from 2^{q-1} strips $H_{\{c\}_{q-1}}$ by $H_{\{c\}_q} = (M^n H_{\{c\}_{q-1}}) \cap V_{c_q}$,

where $\{c\}_q$ and $\{c\}_{q-1}$ coincide in the first $q-1$ symbols; similarly, $\bar{H}_{\{c\}_q} = (M^n \bar{H}_{\{c\}_{q-1}}) \cap \bar{V}_{c_q}$. The width of $H_{\{c\}_q}$ or $\bar{H}_{\{c\}_q}$ is λ^{-nq} that of the TO.

For $q=q_1$, only the part of the strips $\bar{H}_{\{c\}_{q_1}}$ lying in the TO $O_{1,2}$, $\bar{H}_{\{c\}_{q_1}}^{(1,2)} = \bar{H}_{\{c\}_{q_1}} \cap O_{1,2}$, will escape to the next resonance ν_2 . Clearly, in $\bar{H}_{\{c\}_{q_1}}^{(1,2)}$ one must have $c_{q_1}=0$ for $\nu_2 < \nu_1$ ($O_{1,2}$ crosses \bar{V}_0 , as in Fig. 4) and $c_{q_1}=1$ for $\nu_2 > \nu_1$ ($O_{1,2}$ crosses \bar{V}_1). Thus, the number of strips $\bar{H}_{\{c\}_{q_1}}^{(1,2)}$ is 2^{q_1-1} [see Fig. 6(a)]. It is easy to see from the construction above that $V_{\{c\}_{q_1}}^{(1,2)} \equiv M^{-n_1 q_1} \bar{H}_{\{c\}_{q_1}}^{(1,2)}$ are 2^{q_1-1} “vertical” (v) strips lying in $O_{R,1}$; see Fig. 6(b). These strips form precisely the region of $O_{R,1}$ which performs q_1 rotations in ν_1 and lies in $O_{1,2}$ at the end of the q_1 th rotation; in more detail, for $s=1, \dots, q_1-1$, $M^{n_1 s} V_{\{c\}_{q_1}}^{(1,2)}$ lies in the strip $H_{\{c\}_s}$ in ν_1 , where $\{c\}_{q_1}$ and $\{c\}_s$ coincide in the first s symbols.

All the process above, which started from $O_{R,1}$, can be repeated starting from the set of 2^{q_1-1} h strips $\bar{H}_{\{c\}_{q_1}}^{(1,2)}$ in $O_{1,2}$.

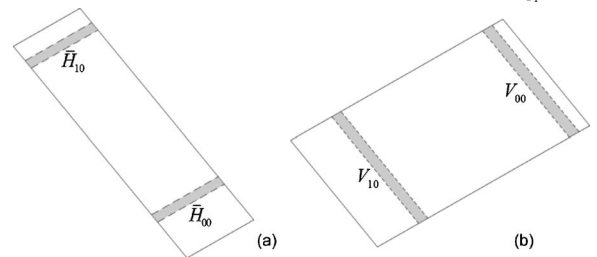


FIG. 6. Schematic illustration, for $q_1=2$, of (a) the h strips $\bar{H}_{\{c\}_{q_1}}^{(1,2)}$ in $O_{1,2}$; (b) the v strips $V_{\{c\}_{q_1}}^{(1,2)}$ in $O_{R,1}$ (see text for more details). In this illustration, $O_{1,2}$ and $O_{R,1}$ correspond to the upper and lower TO, respectively, in Fig. 4.

At the end of the process, each of these strips will split into 2^{q_2-1} substrips, yielding $2^{q_1+q_2-2}$ h strips in $O_{2,3}$; similarly, one obtains $2^{q_1+q_2+q_3-3}$ h strips in $O_{3,4}$, and, finally, 2^{Q_τ} h strips back in $O_{R,1}$. If the process is repeated gR times following g consecutive blocks Γ of τ , one gets 2^{gQ_τ} h strips in $O_{R,1}$. Each strip is naturally denoted by $\bar{H}_{\{c\}_{\tau,g}}$, where $\{c\}_{\tau,g}$ is the sequence of length gC_τ obtained by just combining the gR symbol sequences for the segments visited: $\{c\}_{\tau,g} = \{c\}_{q_1}, \{c\}_{q_2}, \dots, \{c\}_{q_{gR}}$; here we define $q_{r'} = q_r$ for $r' = r + g'R$, with $r = 1, \dots, R$ and $g' = 0, \dots, g-1$. The last symbol in $\{c\}_{q_{r'}}$ is fixed by τ : $c_{q_{r'}} = 0$ for $\nu_{r+1} < \nu_r$ and $c_{q_{r'}} = 1$ for $\nu_{r+1} > \nu_r$. After a careful inspection, it is not hard to verify that $V_{\{c\}_{\tau,g}} \equiv M^{-gT_\tau} \bar{H}_{\{c\}_{\tau,g}}$ ($T_\tau = \sum_{r=1}^R q_r n_r$) is a v strip lying in $O_{R,1}$, as in Fig. 6(b) [30].

Consider now the intersection $I_{\{c,c'\}_{\tau,g}} \equiv \bar{H}_{\{c\}_{\tau,g}} \cap V_{\{c'\}_{\tau,g}}$, where $\{c\}_{\tau,g}$ and $\{c'\}_{\tau,g}$ are any two sequence segments of length gC_τ defined as above. Denoting gC_τ by y for simplicity, we write the combination of the two segments as $\{c\}_{\tau,\pm g} = c_{-y+1}, \dots, c_0, c'_1, \dots, c'_y$, where the y symbols of $\{c\}_{\tau,g}$ are labeled by $i = -y+1, \dots, 0$. Clearly, $I_{\{c,c'\}_{\tau,g}}$ contains the initial conditions (x_0, p_0) for all the orbits of type τ satisfying the following property in the time interval $-gT_\tau \leq t \leq gT_\tau$: When the orbit point (x_t, p_t) visits the principal zone of a resonance, it lies in an H or \bar{H} strip labeled by the symbol sequence c'_1, \dots, c'_i ($i \leq y$) for $t > 0$ and by the symbol sequence c_{-y+1}, \dots, c_i ($i \leq 0$) for $t \leq 0$; the relation between t and i can be easily written in terms of the type. The last symbol (c_i) in the above sequences indicates whether (x_t, p_t) is found on the right ($c_i = 0$) or on the left ($c_i = 1$) of $x = 0$. The bi-infinite sequence $\{c\}_\tau = \lim_{g \rightarrow \infty} \{c\}_{\tau,\pm g}$ is a symbolic representation of the orbit of (x_0, p_0) both forward and backward in time. Since the width of both $\bar{H}_{\{c\}_{\tau,g}}$ and $V_{\{c'\}_{\tau,g}}$ is proportional to λ^{-gT_τ} , $I_{\{c,c'\}_{\tau,g}}$ is a small “box” of area proportional to λ^{-2gT_τ} . Thus, as $g \rightarrow \infty$, $\bar{H}_{\{c\}_{\tau,g}}$ and $V_{\{c'\}_{\tau,g}}$ reduce to two line segments intersecting precisely at (x_0, p_0) . In this way, $\{c\}_\tau$ determines uniquely an orbit of type τ . A PO in $\mathcal{U}_{\tau,l}$ is, of course, represented by a sequence $\{c\}_\tau$ periodic with period lC_τ . For $Q_\tau = 0$, all the symbols in $\{c\}_\tau$ are obviously fixed by τ as described above; then, $\{c\}_\tau$ must be periodic with period $R = C_\tau$ and therefore it corresponds to a PO with $T = T_\tau$. This completes the proof of the statements above concerning the symbolic representation $\{c\}_\tau$.

To derive relation (5), let \mathcal{H}_τ denote the set of initial conditions in $O_{R,1}$ for all the orbits of type τ . We associate with a point (x_0, p_0) in \mathcal{H}_τ the sequence $\{c\}_\tau = \dots, c_{i-1}, c_i, \dots$ representing the corresponding orbit. Obviously, \mathcal{H}_τ is invariant under the map $M^{\pm T_\tau}$ and the point $M^{\pm T_\tau}(x_0, p_0)$ is associated with the shifted sequence $\dots, c_{i-1 \pm y}, c_{i \pm y}, \dots$ ($y = C_\tau$). Thus, \mathcal{H}_τ is a horseshoe whose dynamics under $M^{\pm T_\tau}$ is topologically conjugate to a shift map by $\pm C_\tau$ in a space of bi-infinite binary sequences. It is clear from above that, for any given g , \mathcal{H}_τ is covered by the set of all the intersections $\bar{H}_{\{c\}_{\tau,g}} \cap V_{\{c'\}_{\tau,g}}$ for arbitrary sequences $\{c\}_{\tau,g}$ and $\{c'\}_{\tau,g}$. The number of these intersections is 4^{gQ_τ} and each of them is a box of width/length proportional to λ^{-gT_τ} . Thus, \mathcal{H}_τ is a fractal set whose Hausdorff dimension \bar{D}_τ is determined by $4^{gQ_\tau} \lambda^{-\bar{D}_\tau g T_\tau} = 1$. This gives relation (5).

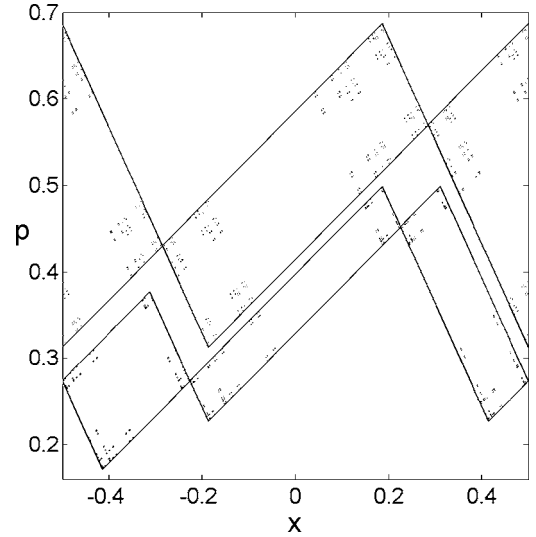


FIG. 7. Solid lines: Resonances $\nu=1/2$ and $\nu'=1/3$ for $K=0.65$. Dots: POs of type τ with basic block $\Gamma(0)=(1/2)_6, (1/3)_8$ ($P_\tau=0$) and $l=1$; one has $T_\tau=36$, $h_\tau=0.231$, and $\bar{D}_\tau=0.588$.

As a matter of fact, an orbit of type τ is represented and uniquely determined by a sequence $\{c\}_\tau$ quite generally, i.e., also when the TOs $O_{r,r+1}$ are not parallelograms. This is because by knowing τ and the c code one can easily calculate the well-known b code $\{b\}$ [9,10,12] which determines uniquely an orbit of the SM; see how $\{b\}$ and $\{c\}_\tau$ are connected in a simple case of τ in Ref. [12]. In general, however, the symbols c do not assume the values $c=0,1$ independently as above. The topological entropy (3) is then smaller than (4). An example of POs of type τ for which all the TOs are parallelograms is shown in Fig. 7; the POs were calculated using their known formulas in terms of $\{b\}$ [10], together with the connection between $\{b\}$ and $\{c\}_\tau$.

IV. DIFFUSION OF ORBITS TRAPPED IN A PERIODIC SET OF RESONANCES

We now derive exact results concerning the diffusion of orbits trapped in a set \mathcal{S} of resonances given by $m_w/n_w + u$, for $w=1, \dots, W$ and for all integers u ; this set is periodic in the p direction and we assume, for definiteness and without loss of generality, that $0 \leq \nu_w = m_w/n_w < 1$ and $\nu_w < \nu_{w'}$ for $w < w'$. The following condition will be imposed on \mathcal{S} : For some integer $J > 0$, the lower turnstile of resonance $\nu_w + J$ has a parallelogram overlap with the turnstile of resonance ν_1 ; from (2), this condition holds for K satisfying

$$K \geq 2J + 2|p_{\nu_w} - p_{\nu_1}| + \frac{K}{\lambda^{n_w} - 1} + \frac{K}{\lambda^{n_1} - 1}. \quad (6)$$

Then, obviously, a general resonance $\nu_w + u$ in \mathcal{S} has also a parallelogram TO with any of the $(2J+1)W-1$ resonances $\nu = \nu_1 + u - J, \dots, \nu_w + u + J$, $\nu \neq \nu_w + u$. We shall also assume that J is chosen as large as possible, i.e., that $\nu_w + J + 1$ and ν_1 have no TO or that the TO is not a parallelogram. Then, the type of an orbit trapped in \mathcal{S} will have the general form

$\tau = \dots, (\nu_{w'} + u')_q, (\nu_w + u)_q, \dots$, with bounded $|u - u'| \sim J$; $|u - u'|$ may be slightly larger than J if, e.g., the TO of resonances $\nu_{w'} + u'$ and $\nu_w + u$ is not a parallelogram. We shall, however, restrict our attention to the ensemble $\mathcal{G} = \mathcal{G}(\mathcal{S}, J)$ of orbits featuring only types with $|u - u'| \leq J$. Such an orbit will always “jump” from $\nu_{w'} + u'$ to $\nu_w + u$ by parallelogram TO.

Global diffusion on \mathcal{G} can be systematically approached on the basis of PO subensembles of \mathcal{G} [15], \mathcal{G}_T , with periods T' dividing T (including $T' = T$). From the definition of $\mathcal{U}_{\tau,l}$ in the previous section, we can write $\mathcal{G}_T = \cup_{lT'=T} \mathcal{U}_{\tau,l}$, where τ are orbit types featured by \mathcal{G} . The diffusion coefficient $D_{\mathcal{G}}$ associated with \mathcal{G} is then defined as follows:

$$D_{\mathcal{G}} = \lim_{T \rightarrow \infty} \frac{1}{2T} \frac{\sum_{lT'=T} N(\tau, l) l^2 P_{\tau}^2}{\sum_{lT'=T} N(\tau, l)}, \quad (7)$$

where the limit should be taken using a proper sequence of periods T , as illustrated by the example below. Formula (7) is consistent with the usual definition of a diffusion coefficient, $D = \lim_{t \rightarrow \infty} \langle (p_t - p_0)^2 \rangle_{\mathcal{E}} / (2t)$; it is also manifestly invariant under canonical transformations preserving the periodicity of the map (1) in (x, p) and it is appropriate for a uniformly hyperbolic system like the SM. As shown below, the value of $D_{\mathcal{G}}$ generally depends on \mathcal{G} .

To calculate (7) and to study the diffusion on \mathcal{G} , we first introduce a convenient symbolic dynamics based on the results of the previous section. If an orbit point (x_t, p_t) lies in the principal zone of some resonance, say $\nu_w = m_w/n_w$, its iterate (x_{t+1}, p_{t+1}) will lie either in ν_w or in one of the $(2J+1)W-1$ resonances $\nu = \nu_1 - J, \dots, \nu_{W+J}$, $\nu \neq \nu_w$. In the first case, (x_t, p_t) can be either on the right ($c=0$) or on the left ($c=1$) side of $x=0$. In the second case, the side of $x=0$ on which (x_t, p_t) lies is automatically fixed by ν : $c=0$ for $\nu < \nu_w$ and $c=1$ for $\nu > \nu_w$. Thus, the symbol sequence $\{c\}_{\tau}$ for an orbit in \mathcal{G} can be replaced by a sequence $\{d\} = \dots, d_i, d_{i+1}, \dots$, where each symbol d_i can assume independently $L = (2J+1)W+1$ values $d=0, 1, 2, \dots, L-1$; the first two values, $d=0, 1$, indicate “staying” in the same resonance while $d=2, \dots, L-1$ indicate “jumping” to one of $L-2$ resonances.

It is more convenient to divide the L values of d into $2J+1$ groups, each associated with a jumping index $j = -J, \dots, J$. The first group, with $j=0$, consists of $W+1$ values $d=0, 1, 2, \dots, W$ (corresponding to staying in ν_w or jumping to $\nu = \nu_1, \dots, \nu_w$, $\nu \neq \nu_w$). Each of the other $2J$ groups, with $j \neq 0$, consists of W values (corresponding to jumping from ν_w to $\nu_1 + j, \dots, \nu_w + j$). Then, for a PO in $\mathcal{G} \cap \mathcal{U}_{\tau,l}$, represented by a sequence $\{c\}_{\tau} = \{d\}$ periodic with period lC_{τ} (see previous section), one must have

$$lP_{\tau} = \sum_{i=1}^{lC_{\tau}} j_i, \quad (8)$$

where j_i is the jumping index associated with d_i .

As an example, we consider the case that all the resonances in \mathcal{S} have the same order, $n_w = n$, $w = 1, \dots, W$ [then

$W \leq \phi(n)$, where $\phi(n)$ is the Euler function]. In this case, if the period of a PO sequence $\{d\}$ is $C = lC_{\tau}$, the actual period of the PO is necessarily $T = nC$. The denominator of the fraction in (7) is just equal to L^C . Using (8), we thus see that

$$D_{\mathcal{G}} = \lim_{C \rightarrow \infty} \frac{1}{2nCL^C} \sum_{j_1, \dots, j_C = -J}^J (j_1 + \dots + j_C)^2, \quad (9)$$

where j_i , for each $i = 1, \dots, C$, assumes $W+1$ times the value $j_i = 0$ and W times a nonzero value in the sum. It is easy to see that this sum is equal to

$$\left(\frac{d^2 \Psi(z)}{dz^2} + \frac{d\Psi(z)}{dz} \right)_{z=1}, \quad (10)$$

where $\Psi(z)$ is the generating function

$$\Psi(z) = \left(1 + W \sum_{j=-J}^J z^j \right)^C. \quad (11)$$

Using (10) with (11) in (9), we obtain

$$D_{\mathcal{G}} = \frac{J(J+1)(2J+1)W}{6n[(2J+1)W+1]}. \quad (12)$$

Formula (12) shows a nontrivial dependence of $D_{\mathcal{G}}$ on \mathcal{G} already in this simple case of $n_w = n$ for all w . The factor n in the denominator of (12) represents the attenuation of the diffusion rate as a result of the “horizontal” motion along the resonances.

As a matter of fact, one can consider j_i in this case as a random variable assuming the value $j_i = 0$ with probability $(W+1)/L$ and a value $j_i \neq 0$, $|j_i| \leq J$, with probability W/L . The standard deviation σ^2 of this variable can be easily calculated: $\sigma^2 = 2nD_{\mathcal{G}}$, where $D_{\mathcal{G}}$ is given by (12). It then follows from the central limit theorem that as $C \rightarrow \infty$ the probability distribution of $\sum_{i=1}^C j_i$ approaches a Gaussian distribution with standard deviation $C\sigma^2$. This shows that one has indeed a rigorous diffusion on \mathcal{G} .

The number of POs with periods $T' = nC'$, where C' divides C , is simply L^C . The topological entropy of \mathcal{G} is then

$$h_{\mathcal{G}} = \lim_{C \rightarrow \infty} \frac{1}{nC} \ln(L^C) = \frac{1}{n} \ln(L). \quad (13)$$

The initial conditions for the orbits of \mathcal{G} form a fractal set whose Hausdorff dimension can be calculated in the same way as in (5):

$$\bar{D}_{\mathcal{G}} = \frac{2h_{\mathcal{G}}}{\ln(\lambda)} = \frac{2 \ln(L)}{n \ln(\lambda)}. \quad (14)$$

Figure 8 shows a PO approximation of this fractal set for the trapping in second-order resonances ($n=2$, $W=1$) with $J=1$; the POs were calculated as explained at the end of Sec. III.

The exact results (12)–(14) are independent of K (and therefore constant) in the interval $K_J \leq K < K_{J+1}$, where K_J is the value of K for which the equality holds in (6). For the trapping in the first-order resonances ($n=W=1$), K_J can be easily calculated:

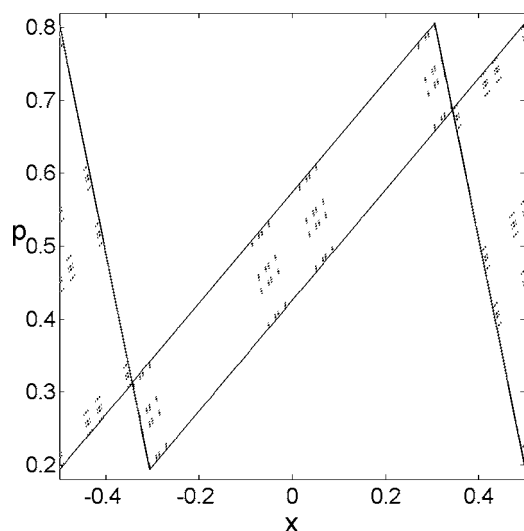


FIG. 8. Solid lines: Resonance $\nu=1/2$ for $K=2.4$. Dots: initial conditions in $\nu=1/2$ for POs with periods $T=2C$ ($C=1, 2, 3, 6$), trapped in the periodic set \mathcal{S} of resonances $\nu=\dots, -1/2, 1/2, 3/2, \dots$. These POs form the sixth approximation level of the fractal ensemble \mathcal{G} trapped in \mathcal{S} with $J=1$ ($L=4$), $h_{\mathcal{G}}=0.6931$, and $\bar{D}_{\mathcal{G}}=0.9726$.

$$K_J = \frac{4(J+2) + 2\sqrt{J^2 + 4J + 1}}{3} - 2. \quad (15)$$

It follows from (15) that in a strong-chaos ($K \gg 1$) regime $K_J \approx 2J+2$, so that, approximately, $K \gtrsim 2J+2$ and $\lambda \gtrsim 2J+4$. Using also $L=2J+2$, this implies that the fractal dimension (14) is very close to 2 from below, i.e., \mathcal{G} is very close to a set of finite measure in phase space. This is consistent with the fact that for $K \gg 1$ most of the phase space is occupied by the first-order resonances [12]. From (12) we find that for $n=W=1$ and $K \gg 1$ (with $J \approx K/2$),

$$D_{\mathcal{G}} \approx \frac{K^2}{24}. \quad (16)$$

We recall that $K^2/24$ is the exact value of the global diffusion coefficient for integer K (cat maps) [8,15] and is an approximate one for all $K \gg 1$ [15,16]. As one could expect, relation (16) shows that this value also well approximates that of (12) for the almost finite-measure ensemble \mathcal{G} .

V. SUMMARY AND CONCLUSIONS

In summary, we have derived rigorous results concerning the quasiregularity and the diffusion of strongly chaotic motion on resonances of the SM. Due to the exact resonance partition in the SM [12], any chaotic orbit is of well-defined quasiregularity type, specifying the sequence of resonances visited by the orbit. We have considered chaotic ensembles of fixed type, involving a finite number R of resonances in the basic torus $0 \leq x, p < 1$. Provided the TOs of consecutively visited resonances are all parallelograms, such an ensemble can be described by a binary symbolic dynamics for which the values of some symbols are fixed by the type and the other symbols take the values 0, 1 independently. The topological entropy and the Hausdorff dimension characterizing the (fractal) ensemble can then be calculated exactly.

A chaotic ensemble trapped in a periodic set of resonances is characterized by a diffusion coefficient depending sensitively on the set considered. The coefficients associated with all such ensembles, generally fractals, give then a much more complete picture of the influence of quasiregularity on chaotic diffusion than a single global coefficient. This is already clearly illustrated by the exact formula (12) in the simple case that all the resonances have the same order. We have shown that the trapped ensemble in this case exhibits a rigorous chaotic diffusion. For first-order resonances, this diffusion approaches the global one in a strong-chaos regime. Thus, one may view this as a rigorous global-diffusion result valid for all $K \gtrsim K_1$, not just for specific (e.g., integer) values of K as in previous works [8,15]. Our exact results may be extended to cases of ensembles trapped in sets of resonances having different orders by using the convenient symbolic dynamics introduced in Sec. IV.

The quantized SM has attracted much attention recently in several contexts [17–20]. It would be interesting to investigate the fingerprints of our classical results in the quantum properties in a semiclassical regime; for example, “scars” of wave functions on POs exhibiting a clear quasiregularity pattern and a possible relation between dynamical localization of quasienergy states on a periodic set of resonances and the diffusion rate of chaotic ensembles trapped in this set.

ACKNOWLEDGMENTS

This work was partially supported by the Israel Science Foundation (Grant No. 118/05).

- [1] B. V. Chirikov, *Phys. Rep.* **52**, 263 (1979); J. D. Meiss, J. R. Cary, C. Grebogi, J. D. Crawford, A. N. Kaufman, and H. D. I. Abarbanel, *Physica D* **6**, 375 (1983); C. F. F. Karney, *ibid.* **8**, 360 (1983); J. D. Meiss and E. Ott, *ibid.* **20**, 387 (1986).
 [2] G. M. Zaslavsky, *Phys. Rep.* **371**, 461 (2002), and references therein.
 [3] O. Barash and I. Dana, *Phys. Rev. E* **71**, 036222 (2005).
 [4] V. A. Rokhlin, *Izv. Akad. Nauk SSSR, Ser. Mat.* **25**, 499 (1961).

- [5] B. V. Chirikov, USSR Academy of Sciences (Siberian Section), Rep. No. 267, CERN Translation Rep. No. 71-40, 1969 (unpublished).
 [6] S. Aubry, in *Soliton and Condensed Matter Physics*, edited by A. Bishop and T. Schneider (Springer-Verlag, New York, 1978), p. 264.
 [7] I. C. Percival, in *Nonlinear Dynamics and the Beam-Beam Interaction*, edited by M. Month and J. C. Herrera, AIP Conf. Proc. No. 57 (AIP, New York, 1979), p. 302.

- [8] J. R. Cary and J. D. Meiss, Phys. Rev. A **24**, 2664 (1981).
- [9] I. C. Percival and F. Vivaldi, Physica D **27**, 373 (1987).
- [10] N. Bird and F. Vivaldi, Physica D **30**, 164 (1988).
- [11] I. Dana, N. W. Murray, and I. C. Percival, Phys. Rev. Lett. **62**, 233 (1989).
- [12] Q. Chen, I. Dana, J. D. Meiss, N. W. Murray, and I. C. Percival, Physica D **46**, 217 (1990).
- [13] I. Dana, Phys. Rev. Lett. **64**, 2339 (1990).
- [14] I. Dana, Phys. Rev. Lett. **70**, 2387 (1993).
- [15] I. Dana, Physica D **39**, 205 (1989).
- [16] R. Artuso and R. Strepparava, Phys. Lett. A **236**, 469 (1997).
- [17] F. Borgonovi, G. Casati, and B. Li, Phys. Rev. Lett. **77**, 4744 (1996); G. Casati and T. Prosen, Physica D **131**, 293 (1999).
- [18] F. Borgonovi, Phys. Rev. Lett. **80**, 4653 (1998).
- [19] G. Benenti, G. Casati, S. Montangero, and D. L. Shepelyansky, Phys. Rev. Lett. **87**, 227901 (2001); Eur. Phys. J. D **22**, 285 (2003).
- [20] S. Bettelli and D. L. Shepelyansky, Phys. Rev. A **67**, 054303 (2003).
- [21] J. Krug, Phys. Rev. Lett. **59**, 2133 (1987).
- [22] P. Ashwin, Phys. Lett. A **232**, 409 (1997).
- [23] I. Dana, Phys. Rev. E **69**, 016212 (2004), and references therein.
- [24] I. Dana and V. E. Chernov, Phys. Rev. E **67**, 046203 (2003).
- [25] I. Dana and V. E. Chernov, Physica A **330**, 253 (2003); **332**, 219 (2004).
- [26] R. S. MacKay, J. D. Meiss, and I. C. Percival, Physica D **27**, 1 (1987), and references therein.
- [27] J. D. Meiss, Rev. Mod. Phys. **64**, 795 (1992), and references therein.
- [28] In Ref. [12], V_0 and V_1 were denoted by \mathcal{V}_2 and \mathcal{V}_1 , respectively.
- [29] All our results in Sec. III trivially extend to $P_\tau \neq 0$ since the TO between resonances $\nu_r + P_\tau$ and $\nu_{r+1} + P_\tau$ is just the translation by P_τ of the TO between ν_r and ν_{r+1} ; for $r=R$, $\nu_{R+1} = \nu_1 + P_\tau$.
- [30] The set $\{V_{\{c\}_{\tau,g}}\}$ develops from map preimages of $\{\bar{H}_{\{c\}_{\tau,g}}\}$ as follows: the set $\{M^{-n_{RR}}\bar{H}_{\{c\}_{\tau,g}}\}$ lies in $O_{R-1,R}$ and is the intersection of $2^{q_{R-1}}$ v strips with $2^{g_{Q\tau+1}-q_R}$ h strips; the set $\{M^{-n_{R-1}q_{R-1}-n_{RR}}\bar{H}_{\{c\}_{\tau,g}}\}$ lies in $O_{R-2,R-1}$ and is the intersection of $2^{q_{R-1}+q_{R-2}}$ v strips with $2^{g_{Q\tau+2}-q_{R-1}-q_R}$ h strips, and so on, until the set of $2^{g_{Q\tau}}$ v strips $\{V_{\{c\}_{\tau,g}}\}$ in $O_{R,1}$ is finally obtained.